Anal. Chem. **1997,** *69,* 2496−2503

Tandem Fourier Transform Mass Spectrometry Studies of Surface-Induced Dissociation of Benzene Monomer and Dimer Ions on a Self-Assembled Fluorinated Alkanethiolate Monolayer Surface

Wenqing Zhong, Eugene N. Nikolaev,† and Jean H. Futrell*

Department of Chemistry and Biochemistry, University of Delaware, Newark, Delaware 19716

Vicki H. Wysocki

Department of Chemistry, University of Arizona, Tucson, Arizona 85721

A new instrument configuration based on a Finnigan FTMS-2000 platform has been applied to the study of surface-induced dissociation (SID) in this research. Benzene monomer ions $C_6H_6^+$ and dimer ions $(C_6H_6)_2^+$ were impacted on a fluorinated self-assembled monolayer surface at collision energies ranging from 1 to 70 eV. Benzene cations were chosen for this study because the fragmentation characteristics of the molecular cation are well known and its SID has been thoroughly investigated. SID spectra obtained by FTMS-SID are very similar to those reported in the literature for the same surface but exhibit much higher mass resolution. A comparison study of collision-induced dissociation (CID) and SID of benzene molecular cations was performed utilizing the same ICR cell and ion detection protocol. It is demonstrated that SID provides both much higher energy deposition and a narrower internal energy distribution than CID. The present instrument geometry and experimental protocol demonstrate much higher efficiencies than previous SID studies by FTMS and much higher mass resolution than previous SID studies using other types of mass analyzers.

High-performance mass spectrometry has emerged as one of the most powerful analytical methods for solving a variety of molecular structure problems. Among high-performance mass spectrometers, Fourier transform mass spectrometry (FTMS) has particular advantages, including high sensitivity, very high mass resolution, high mass accuracy, and essentially unlimited mass range. Extension of mass spectrometry to the analysis of high molecular weight materials, including biopolymers in particular, mainly utilizes “soft” ionization methods such as electrospray ionization (ESI)[1−3] and matrix-assisted laser desorption/ionization (MALDI)[4,5] to generate characteristic ions. Since these techniques mainly generate quasi-molecular ions and very few fragment ions, tandem mass spectrometry has emerged as a key technique for determining connectivity of molecular groups and the structure of large molecules. It therefore follows that tandem high-performance and hybrid spectrometers are uniquely valuable tools for analysis of high molecular weight compounds.

Tandem mass spectrometry commonly utilizes gas phase collision-induced dissociation (CID) of mass-selected ions to generate fragment ions characteristic of the structure of the ion investigated. This has the limitation that energy transfer efficiency in single collisions is limited by momentum transfer and may not be high enough to fragment high-mass ions efficiently, making it difficult to obtain useful structural information for very large ions (e.g., singly charged ions with $m/z > 3500$).[6] Surface-induced dissociation (SID), first introduced by Cooks et al. in 1985,[7−9] is an alternative activation method[10] which has several advantages. These include high internal energy deposition at relatively lower collision energies and deposition of a narrow distribution of energy, leading to high dissociation efficiency.

SID has been successfully applied to high-mass biomolecules,[11] and a variety of SID instrument configurations have been investigated.[12−16] Fourier transfer mass spectrometry combined

---

[†] Present address: Institute of Energy Problems of Chemical Physics, Moscow, Russia.

(1) Fenn, J. B.; Mann, M.; Meng, C. K.; Whitehouse, C. M. *Science* **1989**, *246*, 64.
(2) Fenn, J. B. *J. Am. Soc. Mass Spectrom.* **1993**, *4*, 524.
(3) Dole, M.; Mack, L. L.; Hines, R. L.; Mobley, R. C.; Ferguson, L. D.; Alice, M. B. *J. Chem. Phys.* **1968**, *49*, 2240.
(4) Karas, M.; Bachman, U.; Hillenkamp, F. *Int. J. Mass Spectrom. Ion Processes* **1987**, *78*, 53.
(5) Hillenkamp, F.; Karas, M.; Beavis, R. C.; Chait, B. T. *Anal. Chem.* **1991**, *63*, 1193A.
(6) McCormack, A. L.; Somogyi, A.; Dongre, A. R.; Wysocki, V. H. *Anal. Chem.* **1993**, *113*, 8967.
(7) Mabud, Md. A.; Dekrey, M. J.; Cooks, R. G. *Int. J. Mass Spectrom. Ion Processes* **1985**, *67*, 285.
(8) Cooks, R. G.; Ast, T.; Mabud, Md. A. *Int. J. Mass Spectrom. Ion Processes* **1990**, *100*, 209.
(9) Ast, T.; Mabud, Md. A.; Cooks, R. G. *Int. J. Mass Spectrom. Ion Processes* **1988**, *82*, 131.
(10) Cooks, R. G.; Ast, T.; Pradeep, T.; Wysocki, V. H. *Acc. Chem. Res.* **1994**, *27*, 321.
(11) Dongre, A. R.; Somogyi, A.; Wysocki, V. H. *J. Mass Spectrom.* **1996**, *31*, 339.
(12) Wysocki, V. H.; Ding, J.; Jones, J. L.; Callahan, J. H.; King, F. L. *J. Am. Soc. Mass Spectrom.* **1992,** *3*, 27.
(13) Bier, M. E.; Schwarts, J. C.; Schey, K. L.; Cooks, R. G. *Int. J. Mass Spectrom. Ion Processes* **1990**, *103*, 1.
(14) Williams, E. R.; Fang, L.; Zare, R. N. *Int. J. Mass Spectrom. Ion Processes* **1993**, *123*, 233.

S0003-2700(96)01288-7 CCC: $14.00 © 1997 American Chemical Society

with SID has been briefly explored by Wilkins and co-workers[17] and by McLafferty and co-workers.[18] In these exploratory studies, quasi-molecular ions were mass-selected by standard FTMS methods and excited to high-amplitude trajectories by resonant radio frequency (rf) excitation, causing collision with cell walls or trapping plates. Fragment ions recoiling from these surfaces and injected into the active cell volume are subsequently detected by FTMS. This approach has the advantage that little or no modification to a standard FTMS is required;[17,18] however, the SID excitation process is far from optimized in these experiments. Lack of independent control of key SID parameters leads to low efficiency because of such factors as competition between neutralization and SID (on metal surfaces) and low and unknown efficiency of trapping fragment ions ejected from cell walls or plates. To evaluate SID in combination with FTMS and compare it objectively with other instrument configurations, we have modified an FTMS apparatus to provide independent optimization of both surface composition and collision energy with high efficiency of trapping fragment ions.

Recently, self-assembled monolayer films (SAMs) were shown to have significant advantages as surfaces for SID.[19−23] These films are easily prepared in solution by spontaneous assembly of long-chain alkanethiols onto gold and silver surfaces and are very stable in air. The alkane chains are highly ordered, and covalently bound to the surface through the sulfur. Alkanethiolate films on gold surfaces exhibit a crystalline structure, with the fully extended chains oriented trans zig-zag and tilted at about 30° to the surface normal.[24−26] Wysocki and co-workers[19] have shown that increasing chain length decreases the surface reactivity and reduces the neutralization of ions at the surface. It has also been demonstrated by Wysocki and co-workers[19] and Cooks and co-workers[20,21] that fluorinated alkanethiolate surfaces provide greater energy deposition and much higher efficiency (decreased neutralization) for SID than do alkanethiolate surfaces. For the present study, a fluorinated alkanethiolate surface was used to evaluate SID-FTMS.

Benzene was used as a model compound for evaluating the effectiveness of SID-FTMS. It is a simple molecule with a limited number of fragmentation pathways and has been extensively studied by several groups utilizing quadrupole, sector, and time-of-flight (TOF) mass spectrometers.[8,9,15,19,27−29] Its fragmentation patterns and energy deposition characteristics are well known, and a study of energy transfer efficiency in SID as a function of collision energy in a double-quadrupole mass spectrometer has been carried out by Wysocki and co-workers[30] utilizing the same SAM surface preparation as in the present research.

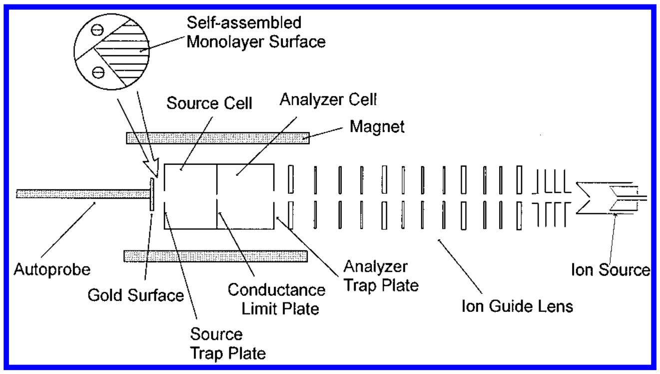

Figure 1. Schematic of modified Finnigan FTMS-2000 external ion source instrument.

EXPERIMENTAL SECTION

Instrumentation. A modified 3 T Finnigan FTMS-2000 Fourier transform mass spectrometer was employed for these experiments.[31] An electrostatic lens external ion source and insertion probe SAM holder whose key features are shown schematically in Figure 1 was used for ion injection and SID with accurate control of ion kinetic energy. Modular ion sources, shown only schematically, currently include EI and CI plasma ion sources and will include an electrospray ion source in future experiments. Electrostatic optics focus and inject ions into the standard dual cell of the FTMS-2000. At present, there is no mass selection of primary ions, and we utilize chemical ionization techniques to generate a known reactant ion. It is planned to incorporate time-of-flight mass selection in a future modification of the apparatus. This dual cell is divided into the analyzer cell and the source cell, separated by a differential pressure aperture. Each cell operates independently and contains two rf excitation plates and two detection plates. Our SID experiments utilized the source cell, which is equipped with an Autoprobe for introducing solid samples. The self-assembled monolayer surface was attached to the Autoprobe as shown in the inset of Figure 1.

A plasma discharge chemical ionization ion source of our own design was used to generate benzene molecular ions and dimer ions. Ions generated by this CI source collide with the surface, and the fragment ions recoil into the source side FTMS cell, where they are trapped and detected by FTMS. It was determined in our experiments that ions are ejected from the surface with relatively low (<4 eV) kinetic energies which were only weakly dependent on primary ion energy. To ensure that fragment ions were injected into the FTMS cell efficiently, we maintained the probe potential at +2 V with respect to the cell trapping plate during ion bombardment. Reflected product ions were trapped

---

(15) de Maaijer-Gielbert, J.; Beijersbergen, J. H. M.; Kistemaker, P. G.; Weeding, T.L. *Int. J. Mass Spectrom. Ion Processes* **1996**, *153*, 119.

(16) Schey, K. L.; Durkin, D. A.; Thornburg, K. R. *J. Am. Soc. Mass Spectrom.* **1995**, *6*, 257.

(17) (a) Ijames, C. F.; Wilkins, C. L. *Anal. Chem.* **1990**, *62*, 1295. (b) Castoro, J. A.; Wilkins, C. L.; Woods, A. S.; Cotter, R. J. *J. Mass Spectrom.* **1995**, *30*, 94.

(18) (a) Williams, E. R.; Henry, K. D.; McLafferty, F. W.; Shabanowitz, J.; Hunt, D. F. *J. Am. Soc. Mass Spectrom.* **1990**, *1*, 413. (b) Chorush, R. A.; Little, D. P.; Beu, S. C.; Wood, T. D.; McLafferty, F. W. *Anal. Chem.* **1995**, *67*, 1042.

(19) Somogyi, A.; Kane, T. E.; Ding, J.-M.; Wysocki, V. H. *J. Am. Chem. Soc.* **1993,** *115*, 5275.

(20) Morris, M.; Riederer, D. E., Jr.; Winger, B. E.; Cooks, R. G.; Ast, T.; Chidsey, C. E. D. *Int. J. Mass Spectrom. Ion Processes* **1992**, *122*, 181.

(21) Winger, B. E.; Julian, R. K., Jr.; Cooks, R. G.; Chidsey, C. E. D. *J. Am. Chem. Soc.* **1991,** *113*, 8967.

(22) Wysocki, V. H.; Jones, J. L.; Ding, J.-M. *J. Am. Chem. Soc.* **1991**, *113*, 8969.

(23) Kane, T. E.; Somogyi, A.; Wysocki, V. H. *Org. Mass Spectrom.* **1993**, *28*, 283.

(24) Porter, M. D.; Bright, T. B.; Allara, D. L.; Chidsey, C. E. D. *J. Am. Chem. Soc.* **1987**, *109*, 3559.

(25) Strong, L.; Whitesides, G. M. *Langmuir* **1988**, *4*, 546.

(26) Finklea, H. O.; Hanshew, D. D. *J. Am. Chem. Soc.* **1992**, *114*, 3173.

(27) Grill, V.; Worgotter, R.; Futrell, J. H.; Mark, T. D. *Z. Phys.D*, submitted.

(28) Schey, K. L.; Cooks, R. G.; Kraft, A.; Grix, R.; Wollnik, H. *Int. J. Mass Spectrom. Ion Processes* **1989**, *94*, 1.

(29) Rosenstock, H. M.; Dannacher, J.; Liebman, J. F. *Radiat. Phys. Chem.* **1982**, *20*, 7.

(30) Vekey, K.; Somogyi, A.; Wysocki, V. H. *J. Mass Spectrom.* **1995**, *30*, 212.

(31) Nikolaev, E.; Rakov, S.; Futrell, J. H.; Ridge, D.; Becker, B.; Winger, B. Campana, J. Presented at the 44th ASMS Conference on Mass Spectrometry and Allied Topics, Portland, OR, May 12−16, 1996; and to be published.

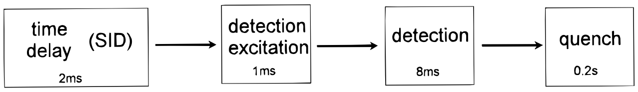

Figure 2. Timing sequence of SID events. During the initial time delay, ions from the cell collide with the surface. Secondary ions coming off the surface are trapped in the cell by lifting the trapping plate to +5 V. Trapping plates are held at this potential during excitation and detection. In the quench pulse, the conductance limit is set to +9.9 V, and trapping plates (and the probe) are set to −9.9 V to sweep ions from the cell before the cycle is repeated.

electrostatically in the cell for FTMS by lifting the trapping plates to +5 V. In some experiments, collisional trapping was employed as an alternative means for capturing SID product ions in the ICR cell by pulsing Ar collision gas into the cell to trap ions by collisional quenching of trapping field motion. The principal reason for investigating two trapping modes for SID fragment ions was to ensure that there was negligible discrimination in the dynamic trapping procedure.

The external source of the instrument illustrated in Figure 1 was utilized in two modes in these experiments. In the normal external ion source sampling mode (sampling mode 1), ions are extracted from the ion source and accelerated to about 1 keV for insertion into the fringing field of the solenoid magnet. They are subsequently decelerated below 5 eV for trapping in the standard dual ICR cell. As described elsewhere by Futrell and co-workers,[32] the source trapping plate is held initially at +5 V, and low-energy ions reverse their trajectories. SIMION modeling demonstrated that this results in a buildup of ion number density in the source section of the dual cell.[32] After time delay sufficient for a steady state to be reached, the conductance limit trapping potential (initially at ground) is raised to +5 V to trap low-energy ions in the cell. Electrostatic trapping and FTMS detection provide reliable sampling of the ion population leaving the external ion source. The second, or SID mode of operation (sampling mode 2) decelerates primary ions to the chosen energy (ranging from 1 to 70 eV in the present experiments) and collides them with the SAM surface on the probe tip, which is located about 1 mm from the source trapping plate. A weak potential difference between the probe tip and source trapping plate migrates low-energy ions into the source cell. The source trapping plate and conductance limit potentials are then lifted to +5 V to trap SID ions. The pulse sequence and timing for both sampling modes are summarized in Figure 2.

CID of benzene ions utilized standard FTMS methods with internal electron impact ionization. The benzene molecular ions were first selected by SWIFT[33] and then excited by resonant excitation. Molecular ions are energized to a preselected translational energy and allowed to undergo collisional activation under single-collision conditions by pulsing Ar into the cell. Fragment ions are then detected in the usual manner. The timing sequence for these experiments is shown in Figure 3.

Surface Preparation. Gold surfaces obtained from Evaporated Metal Films (Ithaca, NY) were fabricated by vapor deposition of gold to a thickness of about 1000 Å on a titanium-coated silica substrate. The gold surface is cleaned by concentrated nitric acid and then immersed in a 1 mM solution of fluorinated alkanethiol for 24 h to form a self-assembled monolayer with the composition $CF_3(CF_2)_9(CH_2)_2SAu$.

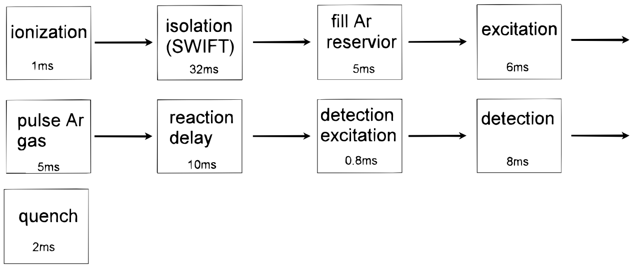

Figure 3. Timing sequence of CID events under a normal operating mode for internal ionization in FTMS. Trapping plates were held at + 4 V throughout the ionization cycles (when the electron gun is pulsed for 1 ms). Stored waveform inverse Fourier transform (SWIFT) was used to isolate the molecular ions. A small-volume (~2 cm^3) reservoir was filled with Ar gas. Selected ions were excited to its terminal kinetic energy at its resonant frequency. Collision gas was admitted into the cell. Fragment ions were detected after collision gas was pumped out of the ICR. Trapping plates were set to −9.9 V during the quench pulse to sweep ions from the cell. The short delay time was chosen, in part, to ensure single-collision condition.

RESULTS AND DISCUSSION

Characterization of Benzene Precursor Ions. Benzene ions are prepared in the plasma CI ion source using a mixture of about 95% Ar with benzene vapor. The sequence of source reactions is as follows:

$$\mathrm{Ar} + \mathrm{e} \rightarrow \mathrm{Ar}^{\bullet+} + 2\mathrm{e} \tag{1}$$

$$\mathrm{Ar}^{\bullet+} + \mathrm{C_6H_6} \rightarrow \mathrm{Ar} + \mathrm{C_6H_6}^{\bullet+}{*} \tag{2}$$

$$\mathrm{C_6H_6}^{\bullet+} + \mathrm{C_6H_6} \rightarrow [\mathrm{C_6H_6}]_2^{\bullet+}{*} \tag{3}$$

$$[\mathrm{C_6H_6}]_2^{\bullet+*} \rightarrow \mathrm{C_6H_6}^{\bullet+} + \mathrm{C_6H_6}{*} \tag{4}$$

$$[\mathrm{C_6H_6}]_2^{\bullet+*} + \mathrm{Ar} \rightarrow [\mathrm{C_6H_6}]_2^{\bullet+} + \mathrm{Ar}{*} \tag{5}$$

where the species in brackets with an asterisk represents benzene dimer ions with sufficient internal energy to dissociate into monomer ion and neutral benzene if they are not stabilized by collision, and the asterisk on Ar indicates energy transfer—in this case as translational energy—which stabilizes the dimer cation. At a low repeller field and total ion source pressure of 2−3 Torr, stabilization reaction 5 is sufficiently rapid that the dimer ion is generated with high efficiency. Increasing the repeller field above 50 Townsend (Td)[34] both decreases the source residence time and modestly enhances the ion kinetic energy as ions drift toward the exit aperture. The combination of collisional "heating" of drifting ions and decreased time for stabilization of the dimer shift the reaction sequence 3−5 back to benzene monomer cation as the major ion leaving the source. The ratio of monomer to dimer ion is readily controlled by adjusting source conditions, and the two different reactant ions—monomer and dimer benzene ions—investigated are low internal energy, essentially "thermalized" reactant ions effusing from a plasma type chemical ionization source.

---

(32) Rakov, S.; Nikolaev, E. N.; Futrell, J. H., to be published.

(33) Marshall, A. G.; Grosshans, P. B. *Anal. Chem.* **1991**, *63*, 215A.

(34) The field gradient and pressure determine the average internal energy, with the mean energy, or effective temperature directly related to the ratio field strength/pressure, which may be expressed in Townsend; see ref 43.

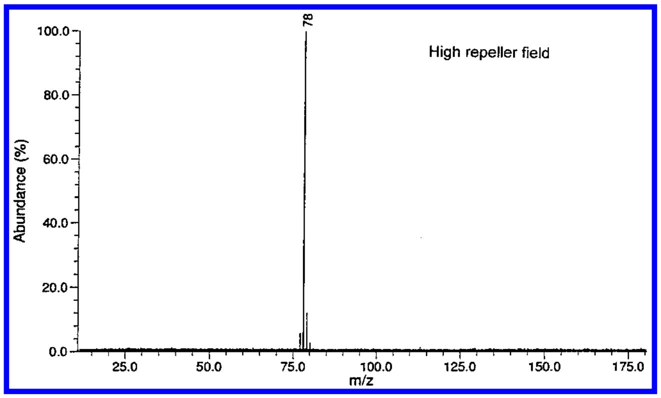

Figure 4. Thermalized benzene molecular ion spectrum obtained with sampling mode 1 (see discussion in text).

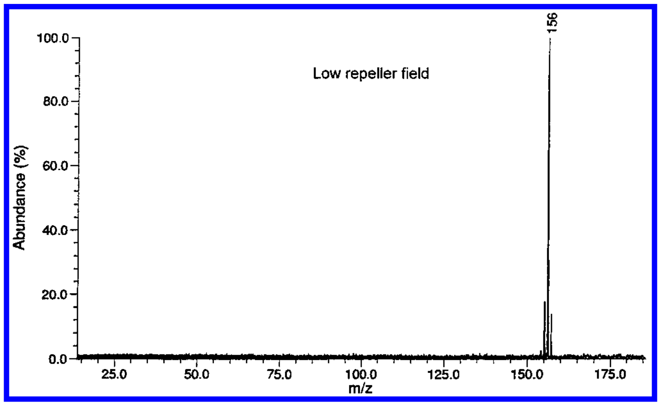

Figure 5. Benzene dimer ion spectrum obtained with sampling mode 2 (see discussion in text).

Figure 4 shows the ion composition for high ion repeller operation of the external ion source at room temperature obtained with sampling mode 1 (described in the Experimental Section). This demonstrates that reactant ions under these conditions are mainly thermalized benzene molecular ions (the *m/z* 79/78 relative ion abundance is the normal abundance ratio for the ^{13}C isotope). Figure 5 shows the composition for “low” repeller field, about 30 Td in this example, also obtained with sampling mode 1. For these source conditions, about 85% of the ions are dimer ions $(C_6H_6)_2^{\bullet+}$ (all of *m/z* 157 is the ^{13}C isotope of the dimer molecular ion), and about 15% are the $C_6H_5{\cdot}C_6H_6^{\bullet+}$ dimer. All the SID experiments reported here were carried out using the source conditions that lead to the spectra shown in either Figure 4 (thermalized molecular ions) or Figure 5 (dimer ions). In subsequent discussions, the reactant ions are described as either monomer or dimer ions, respectively.

Fragmentation of Benzene Monomer Ions. Figure 6 show the SID spectra obtained for 1, 5, 10, 20, 30, and 70 eV collision energy of benzene molecular ions. At 1 eV, the molecular ion recoils from the surface with no dissociation. At 5 eV, low abundances of *m/z* 77 and 52 are detected. At this low collision energy, the *m/z* 39 signal is mainly the second harmonic of the *m/z* 78 signal;[35] any significant contribution from SID can be ruled out on energetic grounds (discussed below). The small extent of fragmentation observed at 5 eV implies that the SID threshold energy for fragmenting thermalized benzene ions is slightly less than 5 eV. At 10 eV, the normalized intensities of these fragment ions are much higher. At 20 and 30 eV, the *m/z* 77 and 52 intensities are of comparable intensity to that of the parent ion. At this energy, *m/z* 39 is too high to be accounted for as second harmonic generation. Significant SID intensity at *m/z* 50, 51, and 63 is also observed. Small adduct peaks are noted as *m/z* 115, 126, 127, and 128. At 70 eV, the parent ion is negligible, and fragmentation is essentially complete. The major SID product ion is *m/z* 50. Ions of *m/z* 39 and 51 are of comparable intensity, followed by *m/z* 63 as a significant SID ion.

Figure 7a presents for comparison SID spectra of benzene ions obtained by Wysocki et al.[19] for the same monolayer surfaces at 30 eV. These results were obtained using a double-quadrupole instrument and 45° ion incidence. Reactant ions were generated by electron impact and are internally excited in comparison with our plasma ion source sampling procedure. Figure 7a spectra are qualitatively similar to those in Figure 6 but differ quantitatively. The most significant difference is the absence of C_2 fragment ions in the present results. The ions $C_2H_2^{\bullet+}$ and $C_2H_3^{\bullet+}$ arise from very high energy fragmentation processes, probably resulting from ring opening and scission reactions; they are very minor reaction products in EI and CID spectra.[29] However, labeling results by Wysocki clearly show that the C_2 fragments originate from SID of benzene and the ions are clearly present in the TOF-SID experiments.[15] Further experiments will explore whether unusual ion energies and scattering angles may be responsible for discrimination against these ions in SID-FTMS experiments at normal incidence.

Figure 7b presents for comparison the 40 ± 5 eV SID spectrum of benzene ions impacted on a Krytox perfluoropolyether surface reported by de Maaijer-Gielbert et al.[15] Reagent ions were formed in these experiments with two photon laser resonant excitation and were both mass-selected and mass-analyzed by TOF-MS. Collision geometry is near normal incidence, and the photoions contain less than 0.5 eV internal energy. Thus, the internal energy and collision geometry are similar; their data most closely resemble those from our 30 eV experiment, with the major difference again being the absence of C_2 fragments.

Kinetic energy dependence of our SID results is readily rationalized from the known thermochemistry and kinetics of benzene ion dissociation processes. The primary ion dissociation steps for benzene molecular ions and energy thresholds for their dissociation are as follows:

$$C_6H_6^{\bullet+} \rightarrow C_6H_5^{\bullet+}(m/z\ 77) + H \qquad \Delta H = 4.73\ \text{eV} \quad (6)$$

$$C_6H_6^{\bullet+} \rightarrow C_4H_4^{\bullet+}(m/z\ 52) + C_2H_2 \qquad \Delta H = 5.52\ \text{eV} \quad (7)$$

The efficiency of conversion of translational energy into internal energy on collision with the fluorinated surface utilized in our research has been estimated by Vekey et al.[30] to be about 28% by a deconvolution of the SID breakdown pattern using the known breakdown graph for unimolecular dissociation of benzene cations. Consequently, we can estimate that the average internal energy deposited in benzene molecular ions is about 1.5 eV at 5 ± 1 eV collision energy. This is much lower than the internal energy required for the fragmentation of benzene ions in the primary decomposition steps 6 and 7. The very low intensities of fragment ions observed in Figure 6 are consistent with this analysis. However, a very small fraction of benzene ions must be excited

---

(35) A detailed discussion of the origin of harmonics in FTMS has recently been published (ref 44). For the same detection protocol and the same ICR cell, the ratio of the second harmonic (*m/z* 39) to the first harmonic (*m/z* 78) should be constant.

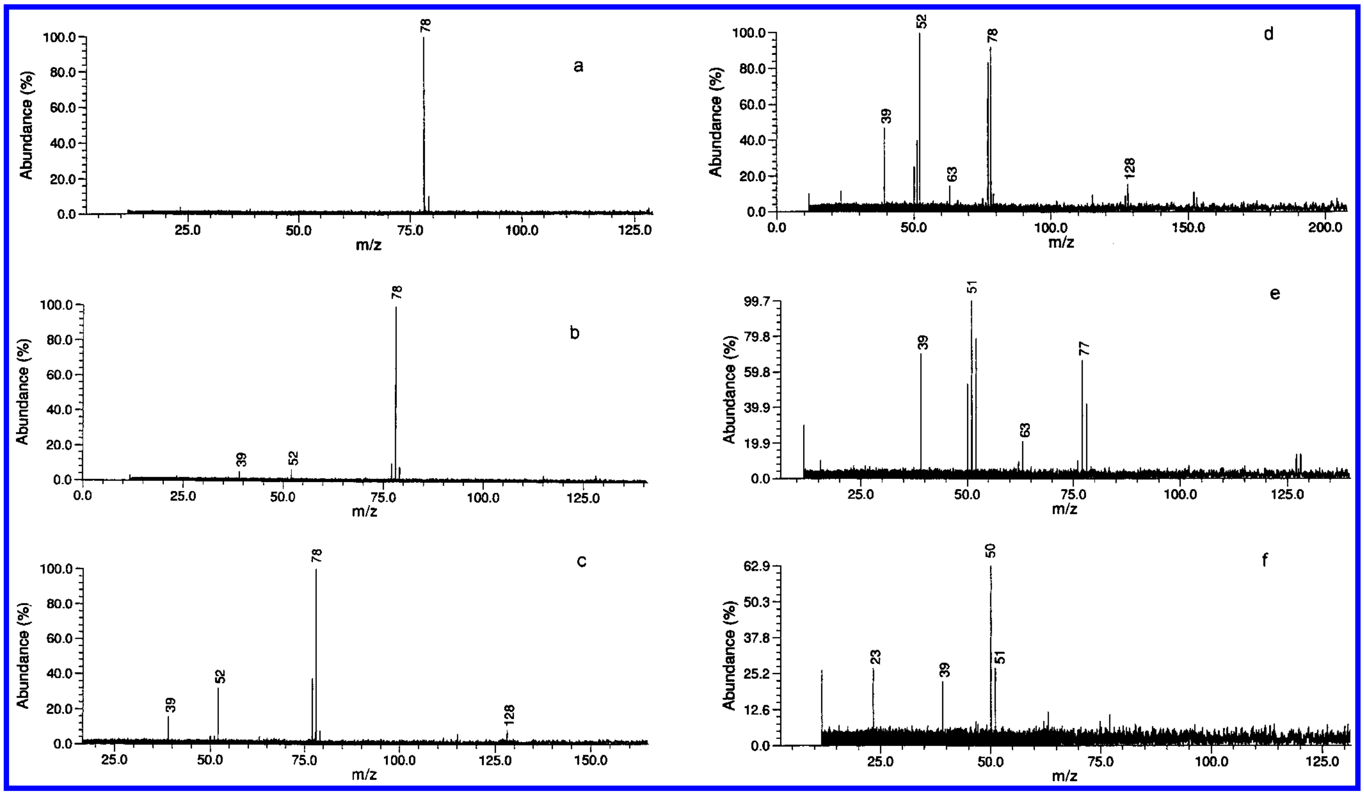

Figure 6. Benzene SID spectra on fluorinated self-assembled monolayer surface obtained at different collision energies: (a) 1, (b) 5, (c) 10, (d) 20, (e) 30, and (f) 70 eV.

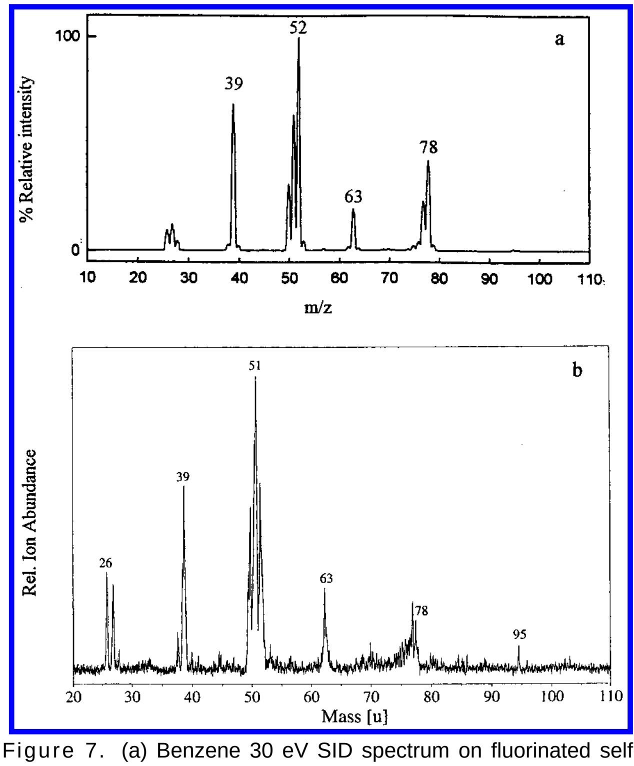

Figure 7. (a) Benzene 30 eV SID spectrum on fluorinated self-assembled monolayer surface obtained by Wysocki and co-workers.[19] (b) Benzene 40 ± 5 eV SID spectrum on Krytox perfluoropolyether surface obtained by de Maaijer-Gielbert et al.[15] Reproduced with permission from ref 15.

to nearly the collision energy to account for the observed fragmentation.

At higher collision energy, SID generates significant ions of *m/z* 50, 51, and 39. These higher energy dissociation processes and their minimum energy requirements[36] are summarized in the following reaction sequences:

$$C_6H_6^{\bullet +} \longrightarrow C_3H_3^{\bullet +}(m/z\ 39) + C_3H_3 \qquad \Delta H = 5.41\text{ eV} \qquad (8)$$

$$C_6H_6^{\bullet +} \longrightarrow C_4H_4^{\bullet +}(m/z\ 52) + C_2H_2$$

$$\hookrightarrow C_4H_3^{\bullet +}(m/z\ 51) + H \qquad \Delta H = 9.2\text{ eV} \qquad (9)$$

$$\hookrightarrow C_4H_2^{\bullet +}(m/z\ 50) + H \qquad \Delta H = 11.9\text{ eV} \qquad (10)$$

With increasing collision energy, more extensive fragmentation is observed, as shown in Figure 6, and the fragment ions from high-energy processes become dominant at 70 eV. The gradual shift is qualitatively, but not quantitatively, consistent with energetic requirements and average conversion efficiency of 30%. In particular, if we assume that no more than 30% of incident ion energy is converted to internal energy, low intensities of high-energy fragment ions are observed below their expected thresholds. Our tentative conclusion, noted earlier, is that some SID collisions result in transfer of significantly more than 30% of the collision energy into internal energy; this hypothesis is consistent with energy distributions that have been reported.[10,30] The previous assertions by these researchers that energy deposition is readily tuned over broad limits by varying collision energy is completely confirmed by the Figure 6 experiments.

Benzene was extensively investigated as a model compound to study ion–surface reaction on SAMs by the Cooks, Bernasek, and Wysocki groups,[10,19,20,37] who have also considered in detail

---

[36] Lias, S. G.; Bartmess, J. E.; Liebman, J. F.; Holmes, J. L.; Levin, R. D.; Mallard, W. G. *Gas-Phase Ion and Neutral Thermochemistry*; National Bureau of Standards: Washington, DC, 1988.

neutralization and reactive collisions on different surfaces under a variety of experimental conditions. Their conclusion that these reactions are minimized for the fluorinated surface $CF_3(CF_2)_7CH_2$-CH_2SAu is the basis of our choice for this surface for SID-FTMS. With the same surface utilized in this research, they report, as minor reaction products, ions of *m/z* 95 and 96, which are initiated by fluorine addition followed by loss of H and H_2, respectively.[19,20] Analogously, peaks at *m/z* 127 and 145 result from addition of CF_3 followed by the loss of HF or H_2. In our spectra, the dominant surface reaction peaks are *m/z* 127 and 128, which may be interpreted as resulting from CF_3 pickup with loss of HF and F (see Figure 6). Adduct ions at *m/z* 95 and 96 were not observed in our experiments.

Detailed mechanistic studies of SID of polyatomic ions on surfaces similar to those used in the present experiments were reported by Hanley et al.[38−40] These researchers utilized high-vacuum techniques of surface scattering to characterize fragment $Cr(CO)_6^+$, iron dicyclopentadienyl $(FeCp_2)^+$, and trimethylsilicon $(SiMe_3)^+$ cations on collision with surfaces on which multilayers of propylene, hexafluoropropylene, and tetrachloroethylene were adsorbed.[39] Consistent with other research summarized above, they demonstrated efficient high translational to internal energy conversion (typically 10%−15% for these small molecules. Their major experimental conclusions were that fragment ions leave the surface with low kinetic energies ($<$4 eV typically, implying that $>$70% of the incident ion energy is dissipated in surface inelastic scattering processes) and are scattered at wide angles (approximately a cosine distribution).

Hanley and co-workers developed a three-step impulsive model to rationalize their observations. On surface impact, impulsive excitation of the incident ion occurs within 10−35 fs. This results in inelastic recoil of the internally excited ion, which subsequently dissociates. Depending on the ions and surfaces investigated, dissociation occurs either before the impacting ion leaves the surface (within 3 ps of impact for $FeCp_2^+$ and $SiMe_3^+$ scattering) or as unimolecular dissociation after the parent ion leaves the surface. The timing of steps 2 and 3 determines whether fragment ions have the same energy or same velocity when they leave the surface. In all cases, the SID reaction occurs very rapidly; this three-step sequence of impulsive excitation, recoil, and dissociation is complete within tens of picoseconds for all cases studied to date.

The TOF study by de Maaijer-Gielbert et al.[15] is consistent with the impulsive mechanism just described. In fact, for TOF-SID-TOF to be effective (in terms of mass resolution), SID reactions must occur with characteristic time scales of tens of picoseconds or less. We assume that essentially the same mechanism applies in our experiments. Because FTMS timing sequences are characteristically in the milliseconds to seconds time scale (see Figures 2 and 3), SID is essentially instantaneous in our experiments. The high efficiency of energy conversion has already been described. Energies of fragment ions leaving the surface are low, estimated to be less than 4 eV in our experiments, and are independent of incident ion energy. This is demonstrated by lifting the source trapping plate to +5 V with respect to the probe tip (see Figure 1) during ion bombardment of the SAM surface, which completely suppresses the SID fragment ion signal, even for 50 eV ion impact on the surface.

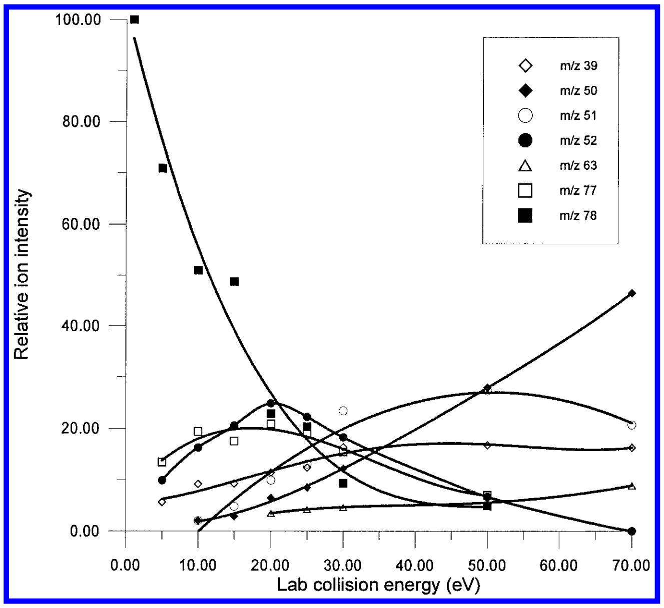

Figure 8. Ion kinetic energy dependence of benzene SID relative ion intensity curve.

Our final method for evaluating benzene cation SID is to compare it quantitatively with gas phase collisional activation. Relative ion intensity curves are presented as a function of ion kinetic energy for both SID and CID in Figures 8 and 9, respectively. Figure 9a shows approximately the same range of laboratory collision energy as Figure 8, while Figure 9b extends the energy range to 1 keV. Energy available in gas phase collisions is governed by the relative, or center-of-mass collision energy,[41] which is obtained in Figure 9 by multiplying E_{lab} by the mass factor $M_{Ar}/(M_{Ar} + M_{benzene})$. It is also well understood that the fragmentation pattern for gas phase CID is only weakly dependent on collision energy above 100 eV collision energy,[41] as clearly shown in Figure 9b for benzene. Since the effective "mass" of the surface impact moiety is unknown, no such comparison is possible in Figure 8. These curves illustrate rather dramatically that energy deposition efficiency is much higher for SID than for CID. It is also evident that a much narrower range of internal energy is deposited in SID activation. Consideration of the detailed kinetic energy dependence in Figure 8 demonstrates that a high degree of selectivity for low-energy versus high-energy fragmentation is possible. Thus, to a significant extent, it is possible to "tune in" internal energy in the benzene cation by changing collision energy.

Benzene Dimer Ion Fragmentation. At lower potential between repeller and source (see Figure 5), benzene dimer cations are the only ions produced in the source by ion−molecule reactions described earlier. The principal species is $(C_6H_6)_2^{\bullet+}$ at *m/z* 156; some 20% of dimer ions are the species $(C_6H_6{\bullet}C_6H_5)^{\bullet+}$ at *m/z* 155. Figure 10 shows the SID spectrum of benzene dimer ions. At 1 eV collision energy, $(C_6H_6)_2^{\bullet+}$ fragments to the monomer ion (Figure 10a). This is the expected result since the binding energy of benzene dimer is only about 0.6 eV.[27] Essentially complete dissociation of the dimer into monomer C_6H_6

---

(37) Hayward, M. J.; Park, F. D. S.; Phelan, L. M.; Bernasek, S. L.; Somogyi, A.; Wysocki, V. H. *J. Am. Chem. Soc.* **1996**, *118*, 8375.

(38) Wu, Q.; Hanley, L. *J. Phys. Chem.* **1993**, *97*, 2677.

(39) Burroughs, J. A.; Wainhaus, S. B.; Hanley, L. *J. Phys. Chem.* **1994,** *98,* 10913.

(40) Burroughs, J. A.; Wainhaus, S. B.; Hanley, L. *J. Chem. Phys.* **1995**, *103*, 6706.

(41) Shukla, A. K.; Futrell, J. H. *Mass Spectrom. Rev.* **1993**, *12*, 211.

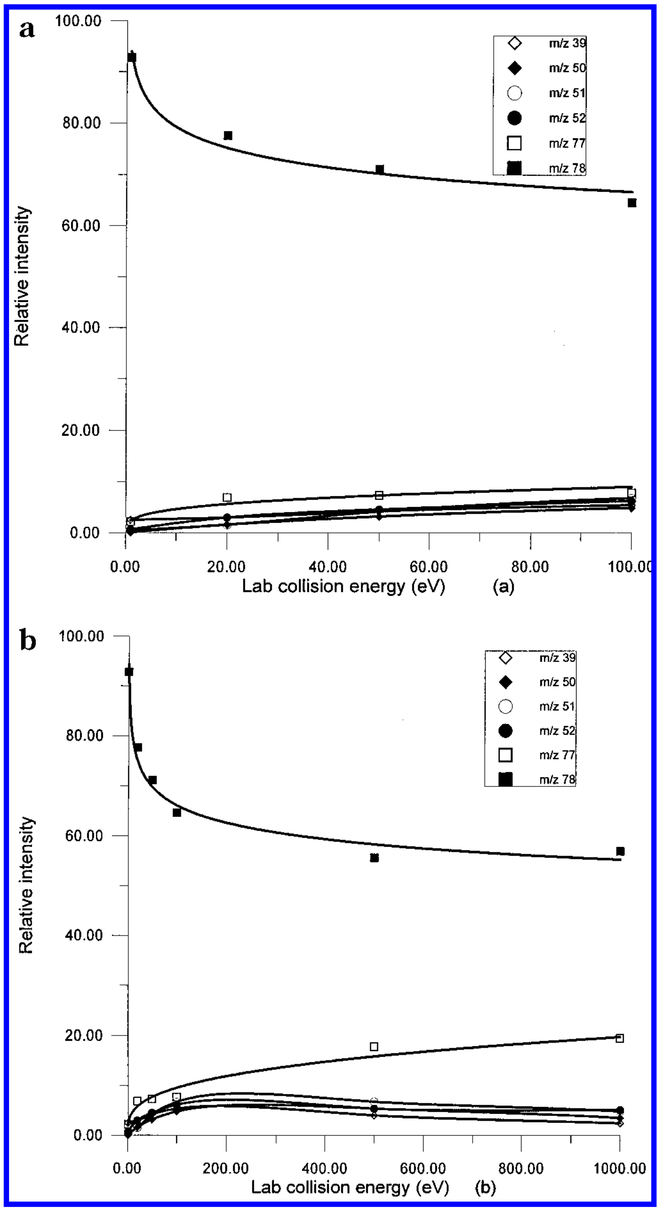

Figure 9. Ion kinetic energy dependence of benzene CID relative ion intensity curve: (a) 1−100 eV lab collision energy; (b) 1−1000 eV lab collision energy.

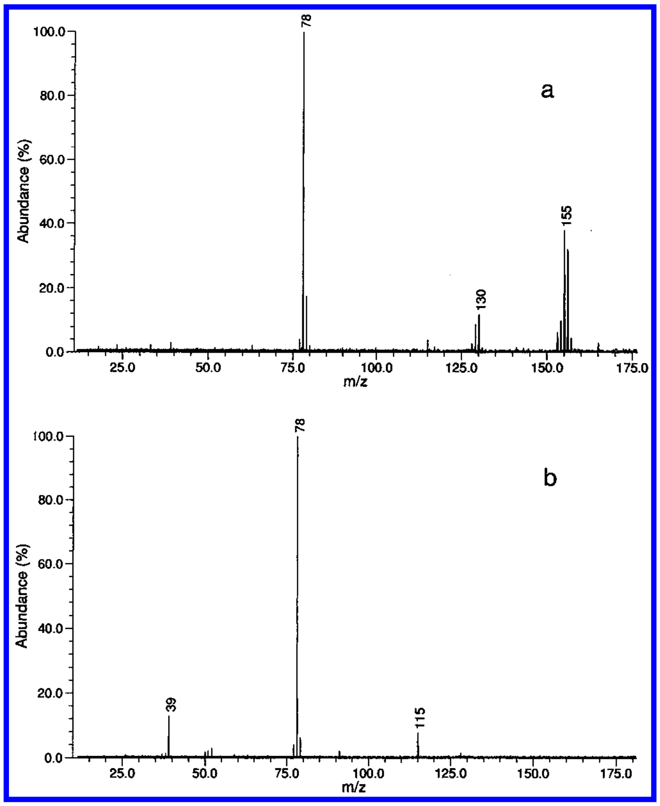

Figure 10. Benzene dimer ions SID spectra on fluorinated self-assembled monolayer surface: (a) 1 and (b) 30 eV.

implies either that the dimers exiting the source contain of the order of 0.3 eV internal energy or that more than 30% of the collision energy is converted into internal energy. We pointed out previously that individual SID spectra suggest an efficiency greater than 30% in a small fraction of surface collisions.

Figure 10 also demonstrates that the intensity of *m/z* 156 $(C_6H_6)_2^{\bullet +}$ decreases very dramatically at 1 eV collision energy while the intensity of *m/z* 155 $(C_6H_6{\bullet}C_6H_5)^{\bullet +}$ remains essentially unchanged. This confirms that the *m/z* 156 ion is the weakly-bound benzene dimer ion while *m/z* 155 ion is covalently bonded. The latter result is in general agreement with results of Grill et al.[27] who impacted benzene cluster ions on a stainless steel surface. The new product ion at *m/z* 130 is $(C_{10}\,H_{10})^{\bullet +}$, most likely resulting from a collision-induced ion-molecule reaction.

At relative high energy (e.g., 30 eV, Figure 10b), benzene monomer further dissociates to fragment ions. We note that the 30 eV SID spectrum of benzene dimer is intermediate in fragmentation behavior to our 10 eV and 20 eV SID spectra of benzene monomer. This is readily explained if dissociation of the weakly bound dimer occurs early in the activation step and subsequent fragmentation of the benzene cation occurs independently of its neutral companion.

Surface Damage by SID. The spot size of the ion beam impacting on the self-assembled monolayer surface has been investigated by Wysocki and co-workers for a double-quadrupole instrument.[42] This experiment was performed by using the so-called condensation figures (CFs) or breath figures technique to visualize the effects of bombarding long-chain alkanethiols with polar terminal groups with 70 eV kinetic energy Ar^+ for 4 h. The damaged area was visualized by the CFs method as a "wetted surface" image, which indicated that the ion beam size was about 9 mm × 8 mm for the quadrupole instrument (for details, see ref 42). In such an instrument, SAM surfaces can be used for several days to study low-energy SID processes for polyatomic cations with no observable degradation in performance. However, in our experiments, the intense magnetic field gives a very sharply focused ion beam at the surface. Changes in the SID spectra and sharp declines in product ion intensity within a few hours were experimental evidence that our SAM surfaces were damaged by benzene ion bombardment. The original spectrum was immediately restored when the probe was rotated by a few degrees to expose an undamaged area to the ion beam. We may infer from this comparison with ref 42 results that the ion beam in our experiments has a spot size somewhat smaller than 2 mm diameter.

---

(42) Kane, T. E.; Angelico, V. J.; Wysocki, V. H. *Anal. Chem.* **1994**, *66*, 3733 (Correction: *Anal. Chem.* **1995**, *67*, 1019).

(43) Mason, E. A.; McDaniel, E. W. *Transport Properties of Ions in Gases*; John Wiley & Sons: New York, 1988.

(44) Nikolaev, E. N.; Rakov, V. S.; Futrell, J. H. *Int. J. Mass Spectrom. Ion Processes* **1996**, *157/158*, 215.

CONCLUSIONS

The results presented in this paper show that surface-induced dissociation combined with FTMS is a very promising method for the analysis of organic molecules. The SID spectra are quite similar to those obtained with other instrument configurations, exhibiting very high energy deposition and extensive fragmentation. At the same time, FTMS gives much higher mass resolution than quadrupole or TOF instruments. The advantages of SID-FTMS will be recognized more fully in the investigation of large biomolecules and polymers, including multiply charged ions. SID in the linear configuration (Figure 1) enables investigation of collision energies down to as low as 1 eV. Combining the tunability and internal energy capabilities of SID with FTMS detection and quantitation has great potential for investigating both fundamental and practical problems in mass spectrometry.

ACKNOWLEDGMENT

Support of this work by the National Science Foundation, Grants CHEM-9021014 (J.H.F.) and CHE9224719 (V.H.W.) is gratefully acknowledged.

Received for review December 19, 1996. Accepted April 4, 1997.⊗

AC9612887

⊗ Abstract published in *Advance ACS Abstracts,* May 15, 1997.